

Article

Transcriptomics Reveals Host-Dependent Differences of Polysaccharides Biosynthesis in *Cynomorium songaricum*

Jie Wang^{1,2}, Hongyan Su³, Hongping Han⁴, Wenshu Wang⁵, Mingcong Li^{1,2}, Yubi Zhou^{1,2,*}, Yi Li^{1,2,*} and Mengfei Li³ 

¹ Qinghai Key Laboratory of Qinghai-Tibet Plateau Biological Resource, Northwest Institute of Plateau Biology, Chinese Academy of Sciences, Xining 810008, China; wangjie@nwipb.cas.cn (J.W.); limingcong@nwipb.cas.cn (M.L.)

² University of Chinese Academy of Sciences, Beijing 100049, China

³ State Key Laboratory of Aridland Crop Science, College of Life Science and Technology, Gansu Agricultural University, Lanzhou 730070, China; Shy922322@163.com (H.S.); lmf@gsau.edu.cn (M.L.)

⁴ School of Chemistry and Chemical Engineering, Qinghai Normal University, Xining 810008, China; sunnyhhp@163.com

⁵ Alxa Forestry and Grassland Research Institute, Alxa 750306, China; amlyswws@163.com

* Correspondence: ybzhou@nwipb.cas.cn (Y.Z.); liyi@nwipb.cas.cn (Y.L.)

Abstract: *Cynomorium songaricum* is a root holoparasitic herb that is mainly hosted in the roots of *Nitraria roborowskii* and *Nitraria sibirica* distributed in the arid desert and saline-alkaline regions. The stem of *C. songaricum* is widely used as a traditional Chinese medicine and applied in anti-viral, anti-obesity and anti-diabetes, which largely rely on the bioactive components including: polysaccharides, flavonoids and triterpenes. Although the differences in growth characteristics of *C. songaricum* between *N. roborowskii* and *N. sibirica* have been reported, the difference of the two hosts on growth and polysaccharides biosynthesis in *C. songaricum* as well as regulation mechanism are not limited. Here, the physiological characteristics and transcriptome of *C. songaricum* host in *N. roborowskii* (CR) and *N. sibirica* (CS) were conducted. The results showed that the fresh weight, soluble sugar content and antioxidant capacity on a per stem basis exhibited a 3.3-, 3.0- and 2.1-fold increase in CR compared to CS. A total of 16,921 differentially expressed genes (DEGs) were observed in CR versus CS, with 2573 characterized genes, 1725 up-regulated and 848 down-regulated. Based on biological functions, 50 DEGs were associated with polysaccharides and starch metabolism as well as their transport. The expression levels of the selected 37 genes were validated by qRT-PCR and almost consistent with their Reads Per kb per Million values. These findings would provide useful references for improving the yield and quality of *C. songaricum*.

Keywords: *Cynomorium songaricum*; polysaccharides biosynthesis; transcriptomics analysis; *Nitraria roborowskii*; *Nitraria sibirica*



Citation: Wang, J.; Su, H.; Han, H.; Wang, W.; Li, M.; Zhou, Y.; Li, Y.; Li, M. Transcriptomics Reveals Host-Dependent Differences of Polysaccharides Biosynthesis in *Cynomorium songaricum*. *Molecules* **2022**, *27*, 44. <https://doi.org/10.3390/molecules27010044>

Academic Editors: Guy P.P. Kamatou and Raffaele Capasso

Received: 31 October 2021

Accepted: 20 December 2021

Published: 22 December 2021

Publisher's Note: MDPI stays neutral with regard to jurisdictional claims in published maps and institutional affiliations.



Copyright: © 2021 by the authors. Licensee MDPI, Basel, Switzerland. This article is an open access article distributed under the terms and conditions of the Creative Commons Attribution (CC BY) license (<https://creativecommons.org/licenses/by/4.0/>).

1. Introduction

Cynomorium songaricum Rupr. is a root holoparasitic herb that is mainly hosted in the roots of *Nitraria* L., and widely distributed in the arid desert and saline-alkaline regions in northwest of China including: Qinghai, Xinjiang, Inner Mongolia and Ningxia [1,2]. As a traditional Chinese medicine, the stem of *C. songaricum* is generally used to tonify kidney yang, replenish essence and blood and relax the bowels [3,4]. In recent years, the stem has also been applied in anti-viral, anti-oxidation, anti-obesity, anti-diabetes, anti-tumor and ameliorates Alzheimer's disease [5–10], which largely rely on the bioactive components including: polysaccharides (mainly polymerized by glucose, mannose and galactose), flavonoids (e.g., catechin, epicatechin and rutin), triterpenes (e.g., ursolic acid, acetyl ursolic acid and malonyl ursolic acid hemiester) and liposoluble constituents (e.g., hexadecanoic acid, oleic acid and docosenoic acid) [5,11–16].

The genus *Nitraria* L. is a perennial shrub and always used as a vital ecological protection plant for windbreak and sand fixation [17]. It contains 11 species in the world and 6 of them are in China [18]. *C. songaricum* is found to mainly host in four species including: *N. roborowskii* Kom., *N. sibirica* Pall., *N. tangutorum* Bobr. and *N. sphaerocarpa* Maxim [19,20]. Except the *N. sphaerocarpa*, the other three species mainly distribute in Qinghai, China [21]. Extensive surveys on habitat have found that *N. roborowskii* prefers locating in the margin of desert, *N. sibirica* in the salinized sand and drought hillslope and *N. tangutorum* is a transitional ecotype between *N. roborowskii* and *N. sibirica* [22,23]. Previous investigations into the differences in growth characteristics between *N. roborowskii* and *N. sibirica* have demonstrated that the growth indexes (e.g., seed weight, fruit weight and seedling height) of *N. roborowskii* are greater than *N. sibirica* [24]; while the salt tolerance, seed-setting rate, contents of nutritional components and trace elements of *N. sibirica* are higher than *N. roborowskii* [25–30].

C. songaricum is currently an endangered species, in large part because of an indiscriminate uprooting of wild plants to meet the increasing commercial demand of the pharmaceutical industry. As a holoparasitic herb, *C. songaricum* totally depends on the *Nitraria* L., for nutrients and water during the whole growth and development cycle [31]. *C. songaricum* is widely used as a traditional Chinese medicine and several pharmacological activities are largely relied on polysaccharides [10,15]; moreover, the growth differences in *C. songaricum* host in the two *N. roborowskii* and *N. sibirica* have been reported [22–24], the regulation mechanism of polysaccharides biosynthesis has not been revealed. Thus, it is urgent and necessary to identify the optimization host to increase production of *C. songaricum*. Up to now, studies on the effect of different hosts on growth and metabolite accumulation of *C. songaricum* have not been conducted. This study examines biomass, soluble sugar accumulation, antioxidant capacity and transcriptional alternations of stem between CR and CS.

2. Results

2.1. Comparison of Growth Characteristics between CR and CS

As shown in Figure 1, significant differences in growth characteristics of stems between the CR and CS were observed, with FW of total stems, FW per stem, stem length and diameter of CR exhibiting a 5.1-, 3.3-, 1.4 and 1.3-fold increase compared to that of CS, respectively.

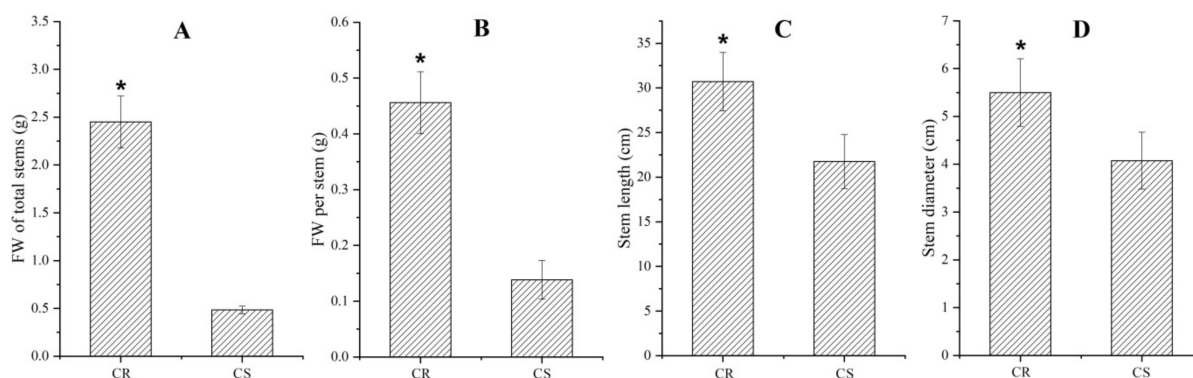


Figure 1. Growth characteristics of stems of *Cynomorium songaricum* host in *Nitraria roborowskii* (CR) and *Cynomorium songaricum* host in *Nitraria sibirica* (CS) (mean ± SD, n = 20). Images (A–D) represent FW of total stems, FW per stem, stem length and diameter, respectively. A t-test was applied for independent samples, the “*” is considered significant at $p < 0.05$ between CR and CS.

2.2. Comparison of Soluble Sugar Content and Antioxidant Capacity between CR and CS

As shown in Figure 2, significant differences in soluble sugar content and antioxidant capacity between the CR and CS were observed, with a 1.1-, 1.5- and 1.5-fold respective decrease of soluble sugar content, DPPH scavenging activity and FRAP value on an FW

basis in stem of CR compared to that of CS (Figure 2A,C,E), while a 3.0-, 2.1- and 2.1-fold increase on a per stem basis (Figure 2B,D,F).

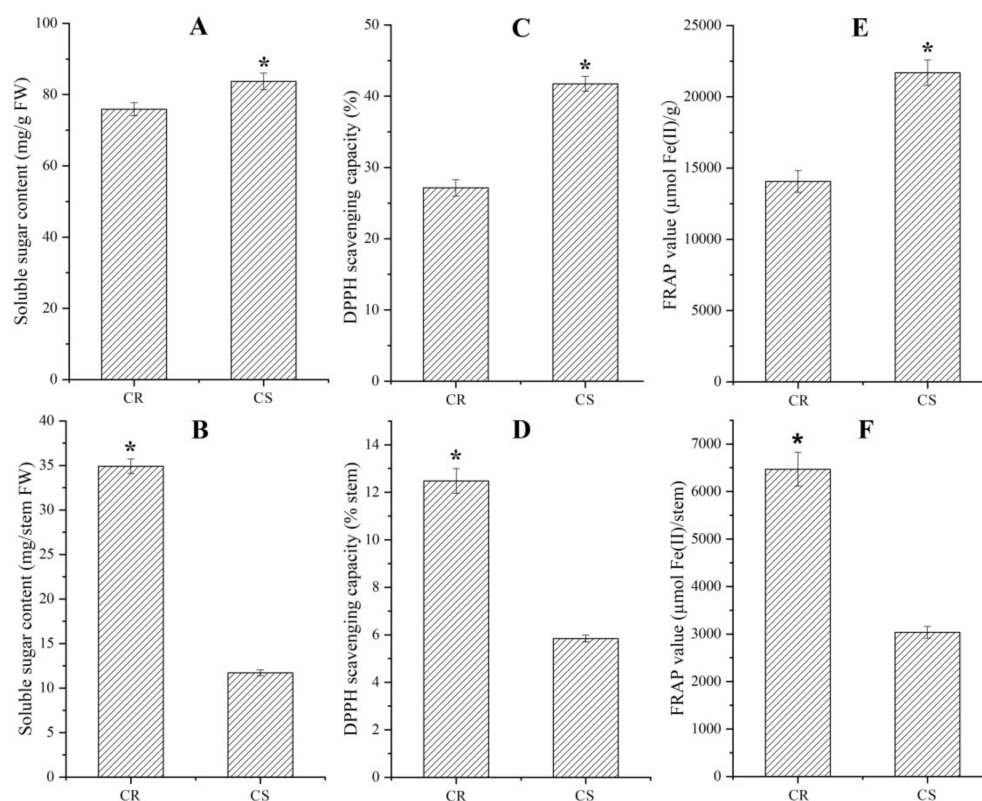


Figure 2. Soluble sugar content and antioxidant capacity in stems between the CR and CS (mean \pm SD, n = 20). Images (A–D) as well as (E,F) represent soluble sugar content, DPPH scavenging activity as well as FRAP value on an FW and per stem basis, respectively. A t-test was applied for independent samples, the “*” is considered significant at $p < 0.05$ between CR and CS.

2.3. Global Gene Analysis

To reveal the differences of carbohydrate metabolism between the CR and CS, comparison of the transcripts were performed. A robust data was collected, 51.2 and 46.8 million high-quality reads were obtained after data filtering, and 42.5 and 39.5 million unique reads as well as 1.6 and 1.4 million multiple reads were mapped from the CR and CS, respectively (Figure 3; Table S1). Total 95,126 unigenes were annotated on KEGG (10,274), KOG (17,550), Nr (40,427) and Swissprot (16,181) databases (Figure 4), and the top 10 species distribution against Nr includes: *Cajanus cajan*, *Vitis vinifera*, *Cephalotus follicularis*, *Theobroma cacao*, *Nicotiana attenuata*, *Juglans regia*, *Corchorus capsularis*, *Brassica napus*, *Brassica rapa* and *Medicago truncatula* (Figure 5).

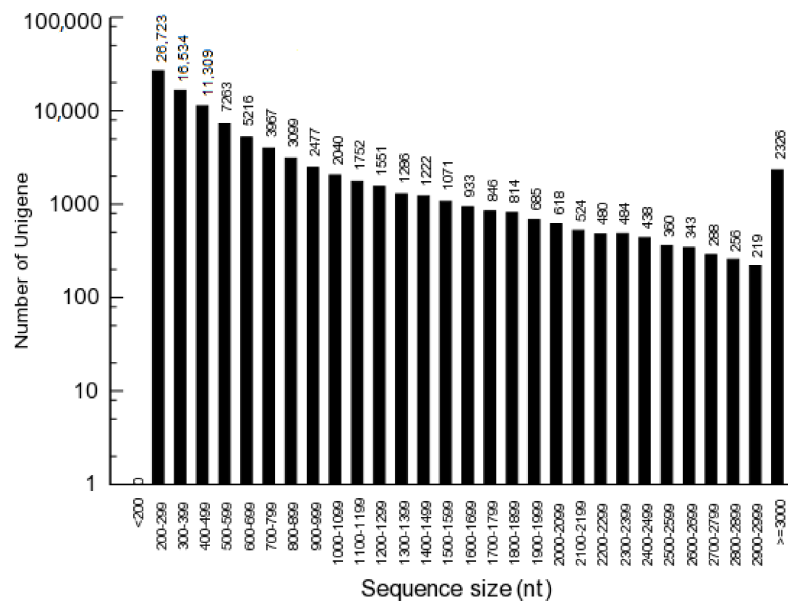


Figure 3. Length distribution of assembled unigenes in *C. songaricum*.

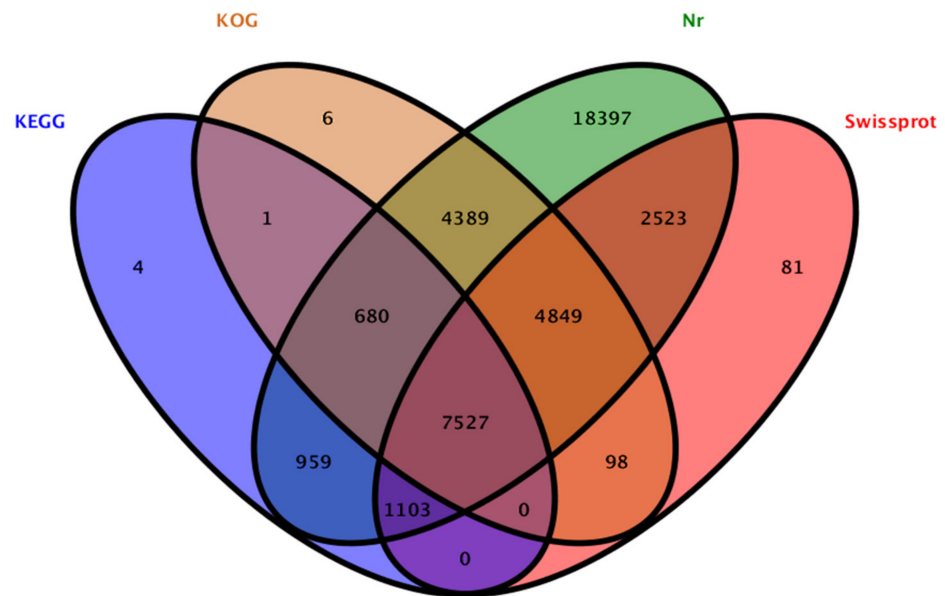


Figure 4. Basic annotation for all unigenes in *C. songaricum* on KEGG, KOG, Nr and Swissprot databases.

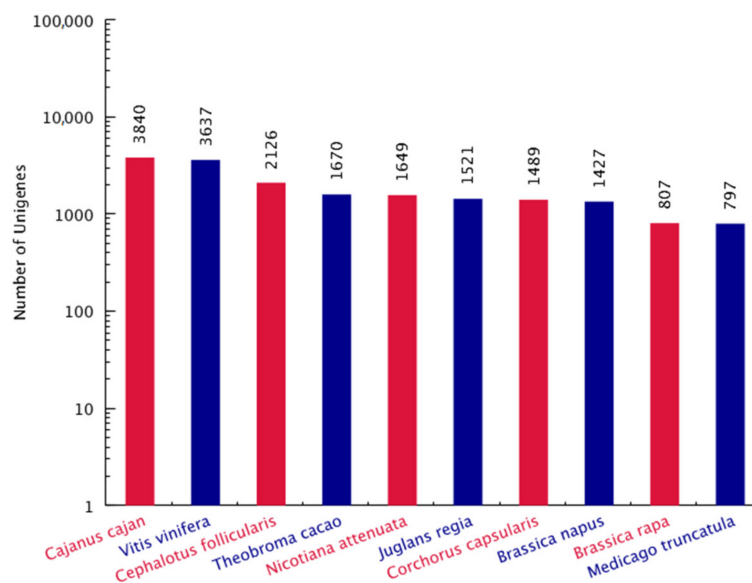


Figure 5. Top 10 species distribution of unigenes against Nr database.

A total of 16,921 DEGs were identified in the CR compared with CS, with 6580 genes up-regulated (UR) and 10,341 genes down-regulated (DR) (Figure 6). Of these 16,921 DEGs, 2684 genes were identified to match with the databases (Figure 7A). Among the 2684 genes, 2573 genes with known functions were partitioned into 1725 UR and 848 DR (Figure 7B,C).

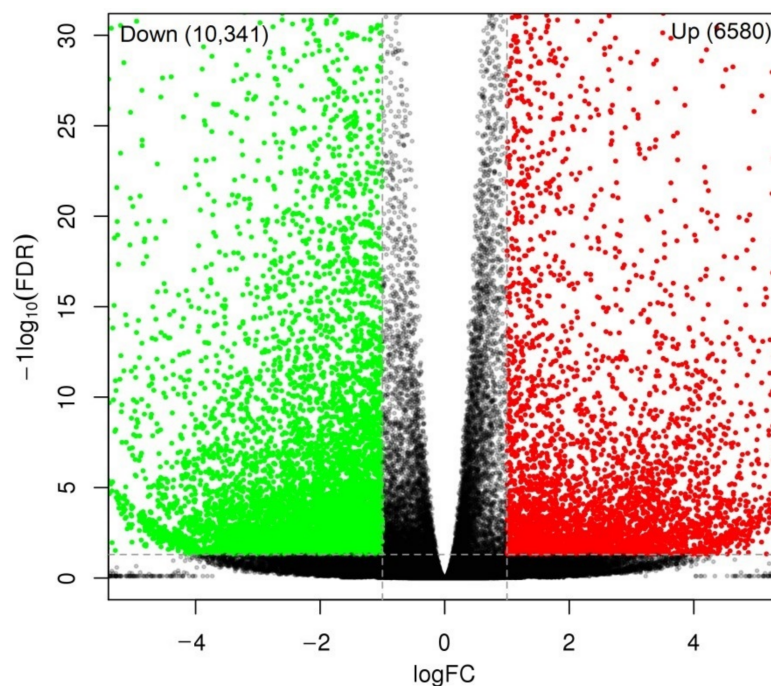


Figure 6. Volcano plot of unigenes and number of differentially expressed genes (DEGs) in the CR compared with CS.

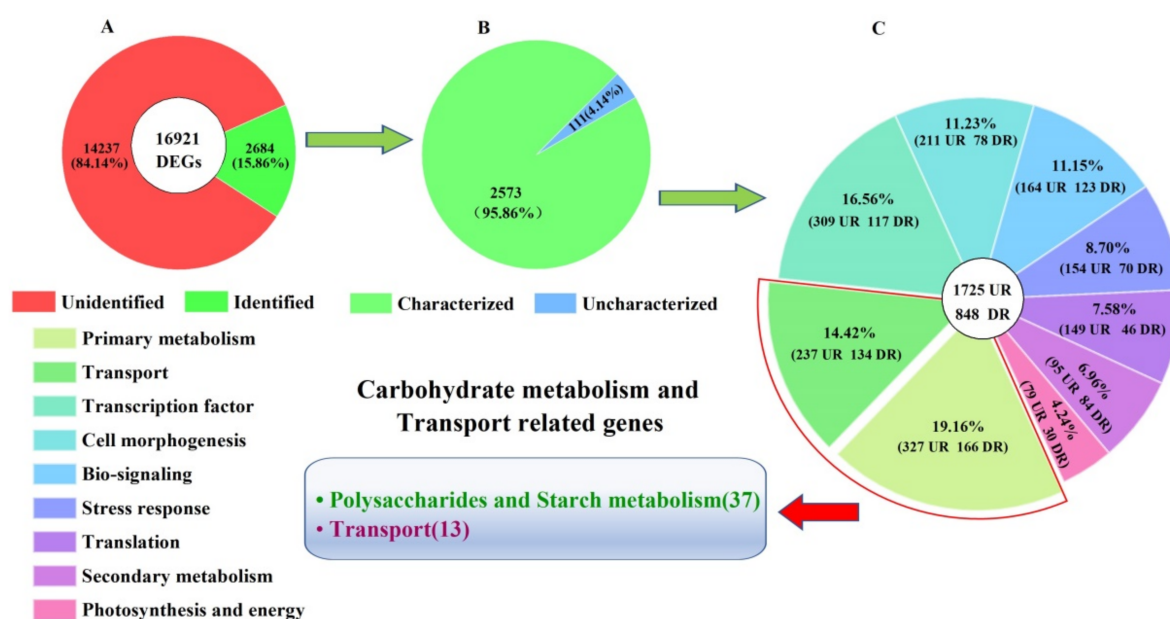


Figure 7. Distribution and classification of DEGs in the CR compared with CS (UR, up-regulation; DR, down-regulation). Image (A) represents the classification of unidentified and identified genes, image (B) represents the classification of uncharacterized and characterized genes and image (C) represents the classification of the functional genes.

2.4. Biological Category of DEGs

Based on biological functions, the 2573 genes were divided into nine categories: primary metabolism (493), transport (371), transcription factor (426), cell morphogenesis (289), bio-signaling (287), stress response (224), translation (195), secondary metabolism (179) and photosynthesis and energy (109) (Figure 7C; Tables S2–S10). Based on carbohydrate metabolism driving genes characterized, 50 DEGs (32UR and 18DR) were identified as potential regulatory genes for polysaccharides and starch metabolism (37) as well as transport (13) (Figure 7C; Table 1).

Table 1. DEGs involved in carbohydrate metabolism and transport in the CR compared with CS.

Gene Name	Swissprot-ID	Protein Name	RPKM (CR/CS)
Polysaccharides Metabolism (32)			
Glucose (7)			
<i>GapA</i>	sp Q8VXQ9 G3PA_COEVA	Glyceraldehyde-3-phosphate dehydrogenase A	8.83
<i>GAPA1</i>	sp P25856 G3PA1_ARATH	Glyceraldehyde-3-phosphate dehydrogenase GAPA1	5.47
<i>GAPA2</i>	sp Q9LPW0 G3PA2_ARATH	Glyceraldehyde-3-phosphate dehydrogenase GAPA2	4.37
<i>GAPB</i>	sp P25857 G3PB_ARATH	Glyceraldehyde-3-phosphate dehydrogenase GAPB	7.25
<i>GAPC</i>	sp P04796 G3PC_SINAL	Glyceraldehyde-3-phosphate dehydrogenase	3.25
<i>PGMP</i>	sp Q9SM59 PGMP_PEA	Phosphoglucomutase	−1.70
<i>UGP1</i>	sp P57751 UGPA1_ARATH	UTP-glucose-1-phosphate uridylyltransferase 1	2.80
Galactose (7)			
<i>BGAL</i>	sp P48981 BGAL_MALDO	Beta-galactosidase	−1.00
<i>BGAL5</i>	sp Q9MAJ7 BGAL5_ARATH	Beta-galactosidase 5	−1.32
<i>BGAL7</i>	sp Q9SCV5 BGAL7_ARATH	Beta-galactosidase 7	−3.29
<i>GALM</i>	sp Q5EA79 GALM_BOVIN	Aldose 1-epimerase	1.34
<i>GALT29A</i>	sp Q9SGD2 GT29A_ARATH	Beta-1,6-galactosyltransferase GALT29A	−3.71
<i>GLCAT14A</i>	sp Q9FLD7 GT14A_ARATH	Beta-glucuronosyltransferase GlcAT14A	−1.10
<i>GOLS2</i>	sp C7G304 GOLS2_SOLLC	Galactinol synthase 2	−1.23

Table 1. Cont.

Gene Name	Swissprot-ID	Protein Name	RPKM (CR/CS)
Mannose (6)			
<i>CYT1</i>	sp O22287 GMPP1_ARATH	Mannose-1-phosphate guanylyltransferase 1	3.29
<i>GMD1</i>	sp Q9SNY3 GMD1_ARATH	GDP-mannose 4,6 dehydratase 1	2.98
<i>MAN5</i>	sp P93031 GMD2_ARATH	Mannan endo-1,4-beta-mannosidase 5	3.21
<i>MSR2</i>	sp Q6YM50 MAN5_SOLLC	Protein MANNAN SYNTHESIS-RELATED 2	1.72
<i>MUR1</i>	sp Q0WPA5 MSR2_ARATH	GDP-mannose 4,6 dehydratase 2	1.24
<i>PMI2</i>	sp Q9FZH5 MPI2_ARATH	Mannose-6-phosphate isomerase 2	1.61
Fucose (5)			
<i>OFUT9</i>	sp Q8H1E6 OFUT9_ARATH	O-fucosyltransferase 9	1.16
<i>OFUT20</i>	sp O64884 OFT20_ARATH	O-fucosyltransferase 20	−2.52
<i>OFUT23</i>	sp Q9MA87 OFT23_ARATH	O-fucosyltransferase 23	−1.86
<i>OFUT27</i>	sp Q8GZ81 OFT27_ARATH	O-fucosyltransferase 27	−1.19
<i>OFUT35</i>	sp Q94BY4 OFT35_ARATH	O-fucosyltransferase 35	1.14
Trehalose (5)			
<i>TPS7</i>	sp Q9LMI0 TPS7_ARATH	Probable alpha,alpha-trehalose-phosphate synthase	−1.40
<i>TPS9</i>	sp Q9LRA7 TPS9_ARATH	Probable alpha,alpha-trehalose-phosphate synthase	8.76
<i>TPS11</i>	sp Q9ZV48 TPS11_ARATH	Probable alpha,alpha-trehalose-phosphate synthase	3.34
<i>TPPF</i>	sp Q9SU39 TPPF_ARATH	Probable trehalose-phosphate phosphatase F	2.27
<i>TPPJ</i>	sp Q5HZ05 TPPJ_ARATH	Probable trehalose-phosphate phosphatase J	2.48
Fructose (2)			
<i>CWINV1</i>	sp Q43866 INV1_ARATH	Beta-fructofuranosidase, insoluble isoenzyme CWINV1	1.40
<i>CYFBP</i>	sp Q9MA79 F16P2_ARATH	Fructose-1,6-bisphosphatase	2.29
Starch Metabolism (5)			
<i>At2g31390</i>	sp Q9SID0 SCRK1_ARATH	Probable fructokinase-1	2.93
<i>DSP4</i>	sp G4LTX4 DSP4_CASSA	Phosphoglucan phosphatase DSP4, amyloplastic	−1.95
<i>NANA</i>	sp Q9LTW4 NANA_ARATH	Aspartic proteinase NANA	−3.64
<i>SBE2.2</i>	sp Q9LZS3 GLGB2_ARATH	1,4-alpha-glucan-branching enzyme 2-2	−1.79
<i>SS2</i>	sp Q43847 SSY2_SOLTU	Granule-bound starch synthase 2	4.05
Carbohydrate Transport (13)			
<i>At1g67300</i>	sp Q9FYG3 PLST2_ARATH	Probable plastidic glucose transporter 2	1.12
<i>ERD6</i>	sp O04036 ERD6_ARATH	Sugar transporter ERD6	2.47
<i>MST1</i>	sp Q0JCR9 MST1_ORYSJ	Sugar transport protein MST1	−1.09
<i>STP1</i>	sp P23586 STP1_ARATH	Sugar transport protein 1	8.84
<i>STP5</i>	sp Q93Y91 STP5_ARATH	Sugar transport protein 5	−1.29
<i>STP12</i>	sp O65413 STP12_ARATH	Sugar transport protein 12	5.61
<i>STP13</i>	sp Q94AZ2 STP13_ARATH	Sugar transport protein 13	3.28
<i>SWEET5</i>	sp Q9FM10 SWET5_ARATH	Bidirectional sugar transporter SWEET5	2.05
<i>SWEET12</i>	sp O82587 SWT12_ARATH	Bidirectional sugar transporter SWEET12	−2.05
<i>SWEET14</i>	sp Q2R3P9 SWT14_ORYSJ	Bidirectional sugar transporter SWEET14	1.57
<i>SWEET15</i>	sp P0DKJ5 SWT15_VITVI	Bidirectional sugar transporter SWEET15	9.57
<i>UXT2</i>	sp Q8GUJ1 UXT2_ARATH	UDP-xylose transporter 2	1.71
<i>UXT3</i>	sp Q8RXL8 UXT3_ARATH	UDP-xylose transporter 3	−1.81

2.5. DEGs Involved in Carbohydrate Metabolism and Transport

2.5.1. DEGs Involved in Polysaccharides Metabolism

Thirty-two DEGs, presenting 21 UR and 11 DR in the CR compared with CS, directly participate in polysaccharides metabolism including: glucose (*GapA*, *GAPA1*, *GAPA2*, *GAPB*, *GAPC*, *PGMP*, and *UGP1*), galactose (*BGAL*, *BGAL5*, *BGAL7*, *GALM*, *GALT29A*, *GLCAT14A*, and *GOLS2*), mannose (*CYT1*, *GMD1*, *MAN5*, *MSR2*, *MUR1*, and *PMI2*), fucose (*OFUT9*, *OFUT20*, *OFUT23*, *OFUT27*, and *OFUT35*), trehalose (*TPS7*, *TPS9*, *TPS11*, *TPPF*, and *TPPJ*) and fructose (*CWINV1* and *CYFBP*) (Table 1). Here, 22 genes were selected to be validated by qRT-PCR, and their RELs were consistent with the RPKM values, with UR for metabolism of glucose, mannose, trehalose and fructose (Figure 8A–D), while differential

expression for fucose metabolism (UR for the *OFUT9* and DR for the *OFUT20*, *OFUT23* and *OFUT27*) (Figure 8E), and DR for galactose metabolism (Figure 8F).

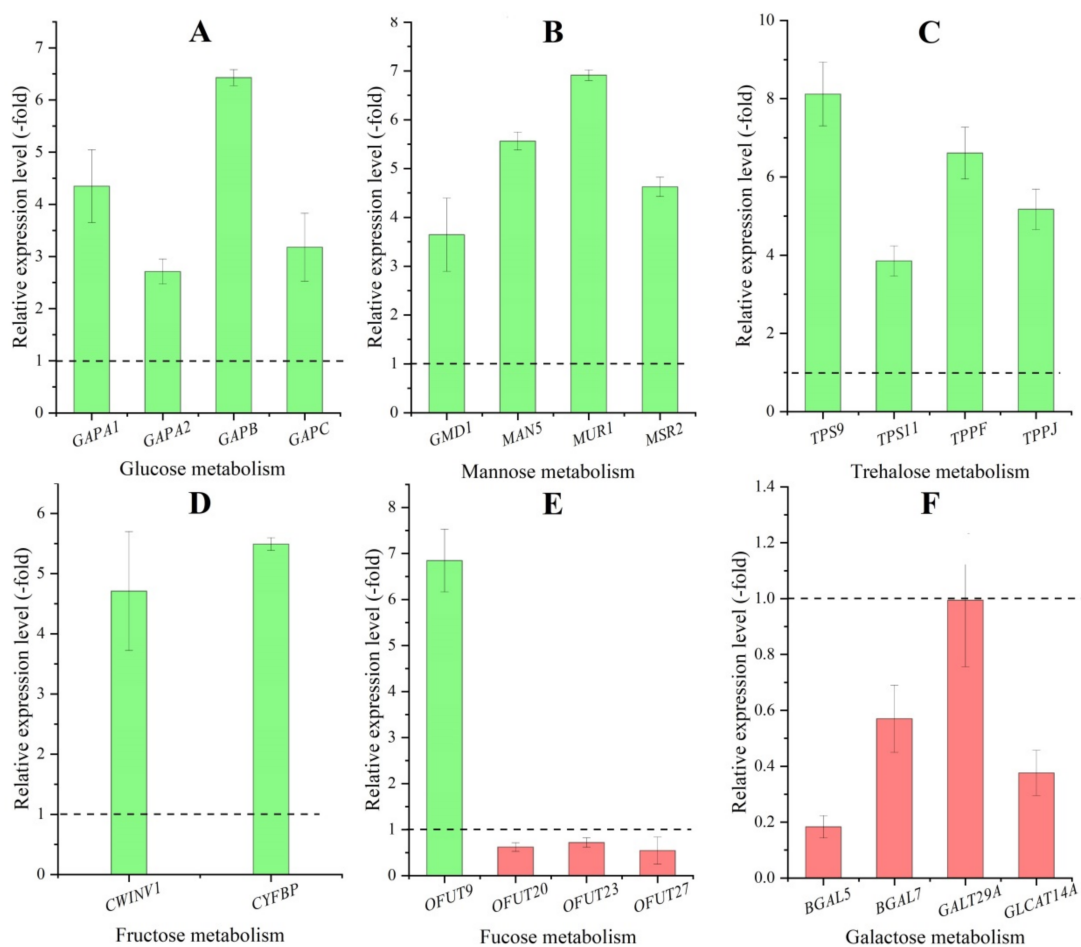


Figure 8. The relative expression level of genes involved in metabolism process of glucose (A), mannose (B), trehalose (C), fructose (D), fucose (E) and galactose (F) in the CR compared with CS, as determined by qRT-PCR. Column highlighted in green represents genes UR and red represents genes DR. The dotted line in the images differentiates UR (>1) and DR (<1) in CR compared with CS, represented. The same below.

2.5.2. DEGs Involved in Starch Metabolism

Five DEGs, presenting two UR and three DR in the CR compared with CS, directly participate in starch metabolism including: *At2g31390*, *DSP4*, *NANA*, *SBE2.2* and *SS2* (Table 1). These genes were validated by qRT-PCR, and their RELs were consistent with the RPKM values, with UR 3.5- and 6.8-fold for the *At2g31390* and *SS2*, and DR 0.6-, 0.9- and 0.6-fold for the *DSP4*, *NANA* and *SBE2.2*, respectively (Figure 9).

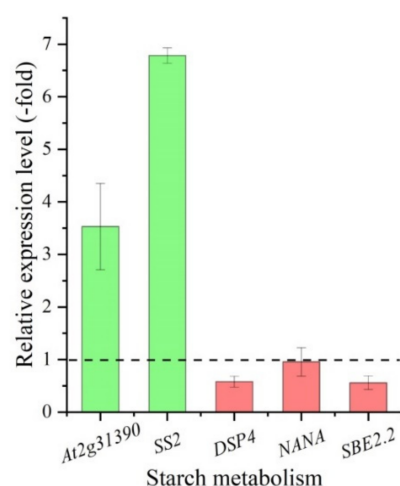


Figure 9. The relative expression level of genes involved in starch metabolism in the CR compared with CS, as determined by qRT-PCR.

2.5.3. DEGs Involved in Carbohydrate Transport

Thirteen DEGs, presenting nine UR and four DR in the CR compared with CS, are involved in carbohydrate transport including: *At1g67300*, *ERD6*, *MST1*, *STP1*, *STP5*, *STP12*, *STP13*, *SWEET5*, *SWEET12*, *SWEET14*, *SWEET15*, *UXT2* and *UXT3* (Table 1). Here, 10 genes were validated by qRT-PCR, and their RELs were consistent with the RPKM values, with the UR 4.5-, 7.3-, 4.6-, 3.5-, 4.5-, 6.2- and 1.5-fold for the *STP1*, *STP12*, *STP13*, *SWEET5*, *SWEET14*, *SWEET15* and *UXT2*, while the DR 0.5-, 0.1- and 0.8-fold for the *STP5*, *SWEET12* and *UXT3*, respectively (Figure 10).

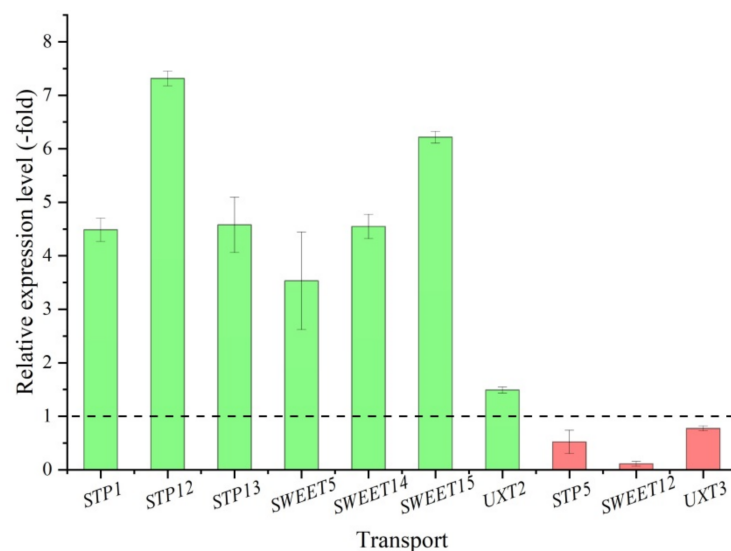


Figure 10. The relative expression level of genes involved in transport in the CR compared with CS, as determined by qRT-PCR.

3. Discussion

Although differences in growth characteristics and nutritional components of *C. songaricum* among the host species, especially in *N. roborowskii* and *N. sibirica*, have been observed in previous studies [25–30], the mechanism responsible for host-dependent growth and bioactive compound biosynthesis has not been dissected. Here, we found that there is a greater biomass, soluble sugar content and antioxidant capacity on a per stem basis in the CR than the CS (Figures 1 and 2). By transcriptomics analysis in the CR compared with CS, a total of 2573 characterized genes differentially expressed with 1725 UR and 848 DR

(Figure 7). By grouping genes based on biological functions, 50 genes (32 UR and 18 DR) were associated with carbohydrate metabolism and transport (Figure 7; Table 1).

Carbohydrates, one of the most abundant and widespread biomolecules in nature, not only plays an important role in plant growth and development, but also represents a treasure trove of untapped potential for pharmaceutical applications [32,33]. In this study, 37 genes were found to be involved in carbohydrate metabolism including polysaccharides (glucose, galactose, mannose, fucose, trehalose and fructose) and starch (Table 1). Among the 37 genes, 23 genes (62%) presenting up-regulated and 14 genes (38%) down-regulated suggest that the level of carbohydrate metabolism is greater in the CR than CS, which is in accordance with the higher content of soluble sugar on a per stem basis in the CR (Figure 2A,B).

For the polysaccharides metabolism, specifically, seven genes associated with glucose metabolic process include: *GapA*, *GAPA1*, *GAPA2*, *GAPB* and *GAPC* participating in the pathway Calvin cycle by catalyzing the reduction of 1,3-diphosphoglycerate by NADPH [34]; *PGMP* participating in both the breakdown and synthesis of glucose [35]; and *UGP1* converting glucose 1-phosphate to UDP-glucose and being essential for the synthesis of sucrose, starch, cell wall and callose deposition [36,37]. Seven genes associated with galactose metabolic process include: *BGAL*, *BGAL5* and *BGAL7* degrading polysaccharides by hydrolyzing terminal non-reducing beta-D-galactose residues in beta-D-galactosides [34]; *GALM* catalyzing the interconversion of beta-D-galactose and alpha-D-galactose [34]; *GALT29A* and *GLCAT14A* involved in the biosynthesis of type II arabinogalactan by, respectively, transferring galactose and glucuronate to oligosaccharides [38,39]; and *GOLS2* involved in the biosynthesis of raffinose family oligosaccharides [38]. Six genes associated with mannose metabolic process include: *CYT1* participating in synthesizing GDP-alpha-D-mannose from alpha-D-mannose 1-phosphate [40]; *GMD1* and *MUR1* catalyzing the conversion of GDP-D-mannose to GDP-4-dehydro-6-deoxy-D-mannose [41]; *MAN5* hydrolyzing the 1,4-beta-D-mannosidic linkages in mannans, galactomannans and glucomannans [42]; *MSR2* involved in mannan biosynthesis [43]; and *PMI2* involved in the synthesis of the GDP-mannose and dolichol-phosphate-mannose required for a number of critical mannosyl transfer reactions [44]. Five genes associated with fucose metabolic process include: *OFUT9*, *OFUT20*, *OFUT23*, *OFUT27* and *OFUT35* participating in the biosynthesis of matrix polysaccharides [45]. Five genes associated with trehalose metabolic process include: *TPS7*, *TPS9*, *TPS11*, *TPPF* and *TPPJ* involved in the trehalose biosynthesis [34,46]. Two genes associated with fructose metabolic process include: *CWINV1* hydrolyzing the terminal non-reducing beta-D-fructofuranoside residues in beta-D-fructofuranosides [47,48]; and *CYFBP* catalyzing fructose-1,6-bisphosphate to fructose-6-phosphate and inorganic phosphate [34,49].

For the starch metabolism, five genes associated with starch metabolic process include: *At2g31390* involved in maintaining the flux of carbon towards starch formation [34]; *DSP4* controlling the starch accumulation and acting as a major regulator of the initial steps of starch degradation at the granule surface [50]; *NANA* regulating endogenous sugar levels (e.g., sucrose, glucose and fructose) by modulating starch accumulation and remobilization [51]; *SBE2.2* involved in starch biosynthesis and catalyzing the formation of the alpha-1, 6-glucosidic linkages in starch [52]; and *SS2* participating in the pathway starch biosynthesis [53].

Transport plays critical roles in distribution and storage of carbohydrate from leaves to roots or other organs that required nutrition [54]. In this study, 13 genes were involved in carbohydrate transport with nine genes (69%) up-regulated and four genes (31%) down-regulated, suggesting that the ability of carbohydrate transport is stronger in the CR than the CS (Table 1). Specially, the 13 genes include: *At1g67300* participating in the efflux of glucose towards the cytosol [55]; *ERD6* participating in sugar transport [56]; *MST1* mediating active uptake of hexoses [57]; *STP1*, *STP5*, *STP12* and *STP13* participating in transporting glucose, 3-O-methylglucose, fructose, xylose, mannose, galactose, fucose, 2-deoxyglucose and arabinose [58]; SWEETs is a unique new family of sugar transporters that lead to

many elusive transport steps including nectar secretion, phloem loading and post-phloem unloading as well as novel vacuolar transporters [59]. Here, four SWEETs genes *SWEET5*, *SWEET12*, *SWEET14* and *SWEET15* participate in phloem loading by mediating export from parenchyma cells feeding H^+ -coupled import into the sieve element/companion cell complex [59,60]; and *UXT2* and *UXT3* participate in transporting UDP-xylose and UMP [61].

4. Materials and Methods

4.1. Plant Materials

Stems of *C. songaricum* at vegetative growth stage, were host in the roots of *N. roborowskii* and *N. sibirica* (Figure 11) were collected on 6 May 2019 from Dulan county (2800 m; 36°2'25" N, 97°40'26" E) of Qinghai, China. The stems were cleaned and rapidly frozen in liquid nitrogen, the middle parts of stem were used for determination of soluble sugar content and antioxidant capacity, and the shoot apical meristems (SAM) were used for transcriptomic analysis.



Figure 11. Morphological characteristics of stems of *C. songaricum* at vegetative growth stage and aerial parts of *N. roborowskii* and *N. sibirica*. Images (A,B) represent stems host in the roots of *N. roborowskii* and *N. sibirica*, and Images (C,D) represent aerial parts of *N. roborowskii* and *N. sibirica*, respectively.

4.2. Measurement of Growth Characteristics

Growth characteristics including fresh weight (FW) of total stems, FW per stem, and its length and diameter were immediately measured after the stems of *C. songaricum* were dug out and cleaned with running water and absorbent paper.

4.3. Determination of Soluble Sugar Content and Antioxidant Capacity

4.3.1. Extracts Preparation

Fresh stems (1.0 g) were ground into homogenate by adding ethanol (20 mL), agitated at 120 r/min and 22 °C for 72 h, then centrifuged at 5000 r/min and 4 °C for 10 min. The supernatant was increased 20 mL with ethanol and then kept at 4 °C for measurement.

4.3.2. Determination of Soluble Sugar Content

Soluble sugar content was determined by a phenol–sulfuric acid method [62,63]. Briefly, extracts (20 μ L) were added in the reaction, absorbance reader was taken at 485 nm and soluble sugar content was calculated based on mg of sucrose.

4.3.3. Determination of Antioxidant Capacity

Antioxidant capacity was determined by DPPH and FRAP methods [64,65]. DPPH radical scavenging assay was determined according to the description of Nencini et al. [66] and Li et al. [63]. Briefly, extracts (5 μ L) were added in the reaction, absorbance reader was

taken at 515 nm and the capacity to scavenge DPPH radicals was calculated as following Equation (1):

$$\text{DPPH scavenging activity (\%)} = [(A_0 - A)/A_0] \times 100 \quad (1)$$

where “ A_0 ” and “ A ” were the absorbance of DPPH without and with sample, respectively.

FRAP assay was determined according to the description of Benzie and Strain [67]. Briefly, extracts (20 μL) were added in the reaction, absorbance reader was taken at 593 nm and the FRAP value was calculated on the basic of ($\text{FeSO}_4 \cdot 7\text{H}_2\text{O}$, 500 $\mu\text{mol Fe (II)/g}$) as following Equation (2):

$$\text{FRAP value (\mu mol Fe(II)/g)} = [(A - A_0)/(A_{\text{FeSO}_4 \cdot 7\text{H}_2\text{O}} - A_0)] \times 500 \text{ (\mu mol Fe(II)/g)} \quad (2)$$

where “ A_0 ” and “ A ” were the absorbance of FRAP without and with sample, respectively; $A_{\text{FeSO}_4 \cdot 7\text{H}_2\text{O}}$ was the absorbance of $\text{FeSO}_4 \cdot 7\text{H}_2\text{O}$.

4.4. Total RNA Extraction, Illumina Sequencing, Sequence Filtration, Assembly, Unigene Expression Analysis and Basic Annotation

Total RNA samples of CR and CS with three biological replicates were extracted using an RNA kit (R6827, Omega Bio-Tek, Inc., Norcross, GA, USA). The processes of enrichment, fragmentation, reverse transcription, synthesis of the second-strand cDNA and purification of cDNA fragments was applied following previous protocols [68]. RNA-seq was performed by an Illumina HiSeqTM 4000 platform (Gene Denovo Biotechnology Co., Ltd., Guangzhou, China). Raw reads were filtered according to previous descriptions [68]. Clean reads were assembled using Trinity [69]. The expression level of each transcript was normalized to RPKM [70], and DEGs were analyzed according to a criterion of $|\log_2(\text{fold-change})| \geq 1$ and $p \leq 0.05$ by DESeq2 software and the edgeR package [71,72]. Unigenes were annotated against the databases including: NR, Swiss-Prot, KEGG, KOG and GO [73].

4.5. qRT-PCR Validation

The primer sequence (Table 2) was designed via a primer-blast in NCBI and synthesized by reverse transcription (Sangon Biotech Co., Ltd., Shanghai, China). First cDNA was synthesized using a RT Kit (KR116, Tiangen, China). PCR amplification was performed using a SuperReal PreMix (FP205, Tiangen, China). Melting curve was analyzed at 72 °C for 34 s. *Actin* gene was used as a reference control. The RELs of genes were calculated using a $2^{-\Delta\Delta\text{Ct}}$ method [74].

Table 2. Sequences of primer employed in qRT-PCR analysis.

Genes	Sequences (5' to 3')	Amplicon Size (bp)
<i>ACT</i>	Forward: CTAAACCGCTTGTTGCTGGC	104
	Reverse: GGGGAGCTCACACGAAAGAT	
Polysaccharides Metabolism (22)		
<i>GAPA1</i>	Forward: TCGTTTTTCATGCTTGTAACCTGT	112
	Reverse: CTTACGCCTCATTTCGCCTC	
<i>GAPA2</i>	Forward: GAAAGCGTCCTGAGCAAAGT	172
	Reverse: GCCCAGGACATACCCAAAAG	
<i>GAPB</i>	Forward: GGCAAGATGGAACTTCATGCG	106
	Reverse: ATGTGAAGTCGGGCCAAAAC	
<i>GAPC</i>	Forward: TTTTGGTCTGAGCCAGAGAGG	106
	Reverse: TGTTACCGCCTGAAAATACCT	

Table 2. Cont.

Genes	Sequences (5' to 3')	Amplicon Size (bp)
Polysaccharides Metabolism (22)		
<i>BGAL5</i>	Forward: AGGCTCTGCTACGTTTGCTT Reverse: TCTCACGTTTCGGCTTTCGT	169
<i>BGAL7</i>	Forward: AGTCTCATTGCCATTCCCCG Reverse: TGGGCGATGAATTTGGTGGGA	104
<i>GALT29A</i>	Forward: AGCTCTGAACGGAAAGCTCAT Reverse: GCTTGCTCACGAATACCCCA	186
<i>GLCAT14A</i>	Forward: TGGTGTGACGAGTTCAAGAGA Reverse: CAGATTCGCTGGTAACTGCCT	148
<i>GMD1</i>	Forward: ATIGCTCTGACACATCACACAC Reverse: GGCTTATAGCGGTCAACAAAAT	101
<i>MUR1</i>	Forward: AGGCAAACGATTGTTGCGAG Reverse: GGATTTGTCAGCCCTTGCTT	180
<i>MAN5</i>	Forward: AGCCAAGAAAATGGCGGAAT Reverse: GCGTGGATGGAATGGTGAAG	198
<i>MSR2</i>	Forward: ACGAGCTTTCTCAAACAGGCA Reverse: TCGCAAGGGCTTCTAAAATGG	153
<i>OFUT9</i>	Forward: GGGTTGTCCTTTGGTCTTGT Reverse: AGTTTGCGCTTGTGTCTACC	110
<i>OFUT20</i>	Forward: TTCAGGACATAGAGGAGCAGC Reverse: GTCCCCCTCCATAAAAGGCG	159
<i>OFUT23</i>	Forward: GCGACTTCTTACCGGCATCT Reverse: GCCTGTCCCAAACCTCTGACA	191
<i>OFUT27</i>	Forward: GTTACCGTTGCAAGACCAC Reverse: CCTTGGCTGGTGAATGGAT	132
<i>TPS9</i>	Forward: TGAGTAAGGAACAAGCCCCATC Reverse: CCTTCCAGGCCGAGACATAA	164
<i>TPS11</i>	Forward: TCCGGTCGGTGAAAGGTATG Reverse: ATCCCATCAACCACAGCCTC	131
<i>TPPF</i>	Forward: TCGGGAAAACCAATGGGTGA Reverse: AGACGGCTGAACTTGAGGTG	128
<i>TPPJ</i>	Forward: TACCAACTGTGCTAAGCCCT Reverse: CTGTATATTGGTTTTGGAAGGC	104
<i>CWINV1</i>	Forward: GTGACGTGTGTTTCCAGTGTG Reverse: TCAGTGTCAGCCATAAGTTGGT	109
<i>CYFBP</i>	Forward: TAGTGGGCAGGGTTTAGGCA Reverse: TCGTGCGGTTAGTGTTTTACCT	109

Table 2. Cont.

Genes	Sequences (5' to 3')	Amplicon Size (bp)
Starch (5)		
<i>At2g31390</i>	Forward: TGTCCGCAAACAGAAAACGTC Reverse: TGGACGCCAAAGAGGGAATG	120
<i>DSP4</i>	Forward: CCCGTGTTTATCCTCGTTGGT Reverse: AAGGTGGTGGTTGACGGTG	157
<i>NANA</i>	Forward: ATGCCGATCCCCAAACACA Reverse: CGAAGGTAATGCCAAATTGAGA	102
<i>SBE2.2</i>	Forward: TGTCCGCAAACAGAAAACGTC Reverse: TGGACGCCAAAGAGGGAATG	120
<i>SS2</i>	Forward: CGGCACAAAATCAACATGGG Reverse: CCAGGCATTGAGTTGCGAAG	104
Transport (10)		
<i>STP1</i>	Forward: GCACTTAGCTTTGATATGCCCC Reverse: TTAAAGACCCATCGCCGTCC	112
<i>STP5</i>	Forward: TCTGAGACAAACAGCCTTCC Reverse: TCCCGTGTATAAGTGCTCTACC	110
<i>STP12</i>	Forward: ACGAGCTCTGCAAAGGGTTC Reverse: CTCCAICTGGTTCAACGCAC	179
<i>STP13</i>	Forward: AGTGTTGACGGGGACTCTT Reverse: ACCCCCTCTTGAGTCTTGTC	146
<i>SWEET5</i>	Forward: GGGTTAGGTTGTCTGGACT Reverse: GCTTTGTCAAGTGTGGTGCT	100
<i>SWEET12</i>	Forward: TCTGACAACACTACCCGCAAGC Reverse: AGGCACAGATAGTTGCCGAA	190
<i>SWEET14</i>	Forward: AGCTGCCGAAAGTACCCTAC Reverse: TCGCATGTTTCTCCTTCGCT	130
<i>SWEET15</i>	Forward: TGTCGCCGTTGCATTTTTGT Reverse: CTCAACTGGGTGGCCTTCAA	137
<i>UXT2</i>	Forward: AGGCCTGATTGCAAGAGCTTA Reverse: CACGGGTACGTCACTCAGAT	148
<i>UXT3</i>	Forward: TGCGGTTAACCTGGAAGAGG Reverse: TGTTTAGGACATCCTCCCATGC	189

4.6. Statistical Analysis

All the measurements were performed using three biological replicates. A *t*-test was applied for independent samples, with $p < 0.05$ considered significant.

5. Conclusions

From the above observations, the stem biomass and polysaccharides accumulation of *C. songaricum* host in *N. roborowskii* are significantly greater than that of *N. sibirica*. A total of 1725 UR and 848 DR genes were observed in CR compared to CS, and 50 DEGs were involved in polysaccharides biosynthesis, which indicates that the polysaccharides

biosynthesis in *C. songaricum* is host-dependent. The specific roles of candidate genes in regulating polysaccharides biosynthesis will require additional studies.

Supplementary Materials: The following are available online. Table supplemental legends: Table S1: Summary of sequencing data for *Cynomorium songaricum* transcriptome; Table S2: Primary metabolism genes differentially expressed in CR and CS; Table S3: Transport genes differentially expressed in CR and CS; Table S4: Transcription genes factor differentially expressed in CR and CS; Table S5: Cell morphogenesis genes differentially expressed in CR and CS; Table S6: Bio-signaling genes differentially expressed in CR and CS; Table S7: Stress response genes differentially expressed in CR and CS; Table S8: Translation genes differentially expressed in CR and CS; Table S9: Secondary metabolism genes differentially expressed in CR and CS; Table S10: Photosynthesis and energy genes differentially expressed in CR and CS.

Author Contributions: J.W. and H.S.: data curation, methodology and writing—original draft. H.H. and M.L. (Mingcong Li): methodology and investigation. W.W.: resources. Y.Z.: project administration and supervision. Y.L.: conceptualization and investigation. M.L. (Mengfei Li) conceptualization and writing—review and editing. All authors have read and agreed to the published version of the manuscript.

Funding: This work was financially supported by the Key Research and Transformation projects of Qinghai Province (2019-SF-171), Local Scientific Development Fund guided by the Central Government of Inner Mongolia (2021ZY0043), and Application Technology Research and Development of Alxa (AMYY2020-11).

Institutional Review Board Statement: Not applicable.

Informed Consent Statement: Not applicable.

Data Availability Statement: The datasets are publicly available at NCBI, with BioSample accession: SAMN13722045 (*Nitraria roborowskii*) and SAMN13722048 (*Nitraria sibirica*), Sequence Read Archive (SRA) accession: SRR10829653 to 10829655 (*Nitraria roborowskii*) and SRR10829660 to 10829662 (*Nitraria sibirica*) (<https://dataview.ncbi.nlm.nih.gov/object/PRJNA598928>). (accessed on 1 February 2021)

Conflicts of Interest: The authors declare no conflict of interest.

Sample Availability: Samples of *Cynomorium songaricum* and other compounds are available from the authors.

Abbreviations

CR	<i>Cynomorium songaricum</i> host in <i>Nitraria roborowskii</i> Kom.
CS	<i>Cynomorium songaricum</i> host in <i>Nitraria sibirica</i> Pall.
DEGs	differentially expressed genes
DPPH	1,1-diphenyl-1-picrylhydrazyl
DR	down regulation
FRAP	ferric reducing antioxidant power
GO	gene ontology
KEGG	Kyoto Encyclopedia of Genes and Genomes
KOG	euKaryotic orthologous groups of proteins
NCBI	National Center for Biotechnology Information
NR	non-redundant protein
REL	relative expression level
RPKM	Reads Per kb per Million
UR	up regulation

References

1. Chinese Academy of Sciences; China Flora Editorial Committee. *Flora Reipublicae Popularis Sinicae*; Science Press: Beijing, China, 2000; Volume 53, pp. 152–154.
2. Cui, J.L.; Gong, Y.i.; Vijayakumar, V.; Zhang, G.; Wang, M.L.; Wang, J.H.; Xue, X.Z. Correlation in chemical metabolome and endophytic mycobiome in *Cynomorium songaricum* from different desert locations in china. *J. Agric. Food Chem.* **2019**, *67*, 3554–3564. [[CrossRef](#)]

3. Liu, H.P.; Chang, R.F.; Wu, Y.S.; Lin, W.Y.; Tisai, F.J. The Yang-Tonifying Herbal Medicine *Cynomorium songaricum* Extends Lifespan and Delays Aging in *Drosophila*. *J. Evid. Based Complement. Altern. Med.* **2012**, *10*, 735481.
4. Committee for the Pharmacopoeia of PR China. *Pharmacopoeia of PR China*; Chinese Medical Science and Technology Press: Beijing, China, 2020; Volume 1, p. 346.
5. Ma, C.M.; Wei, Y.; Wang, Z.G.; Hattori, M. Triterpenes from *Cynomorium songaricum*—Analysis of HCV protease inhibitory activity, quantification, and content change under the influence of heating. *J. Nat. Med.* **2009**, *63*, 9–14. [[CrossRef](#)]
6. Ma, C.M.; Sato, N.; Li, X.Y.; Nakamura, N.; Hattori, M. Flavan-3-ol contents, anti-oxidative and α -glucosidase inhibitory activities of *Cynomorium songaricum*. *Food Chem.* **2010**, *118*, 116–119. [[CrossRef](#)]
7. Chen, J.H.; Wong, H.S.; Leung, H.Y.; Leong, P.K.; Chan, W.M.; Ko, K.M. An ursolic acid-enriched *Cynomorium songaricum* extract attenuates high fat diet-induced obesity in mice possibly through mitochondrial uncoupling. *J. Funct. Foods* **2014**, *9*, 211–224. [[CrossRef](#)]
8. Jin, S.W.; Chen, G.L.; Du, J.J.M.; Wang, L.H.; Ren, X.; An, T.Y. Antioxidant properties and principal phenolic compositions of *Cynomorium songaricum* Rupr. *Int. J. Food Prop.* **2014**, *17*, 13–25. [[CrossRef](#)]
9. Cheng, D.; Su, L.; Wang, X.; Li, X.J.; Li, L.L.; Hu, M.Y.; Lu, Y. Extract of *Cynomorium songaricum* ameliorates mitochondrial ultrastructure impairments and dysfunction in two different in vitro models of Alzheimer's disease. *BMC Complement. Med. Ther.* **2021**, *21*, 206. [[CrossRef](#)]
10. Shi, Z.Q.; Wang, L.Y.; Zheng, J.Y.; Xin, G.Z.; Chen, L. Lipidomics characterization of the mechanism of *Cynomorium songaricum* polysaccharide on treating type-2 diabetes. *J. Chromatogr. B* **2021**, *1176*, 122737. [[CrossRef](#)]
11. Zhou, Y.B.; Ye, R.R.; Lu, X.F.; Lin, P.C.; Yang, S.B.; Yue, P.P.; Zhang, C.X.; Peng, M. GC-MS analysis of liposoluble constituents from the stems of *Cynomorium songaricum*. *J. Pharm. Biomed. Anal.* **2009**, *49*, 1097–1100. [[CrossRef](#)]
12. Luan, N.; Chang, P.; Zhuang, L.Y.; Shang, X.Y. Isolation and determination of catechin from *Cynomorium songaricum* Rupr. *Med. Plant* **2010**, *8*, 87–91.
13. Jin, S.W.; Doi, A.; Kuroda, T.; Zhang, G.X.; Hatano, T.; Chen, G.L. Polyphenolic constituents of *Cynomorium songaricum* Rupr. and antibacterial effect of polymeric proanthocyanidin on methicillin-resistant *staphylococcus aureus*. *J. Agric. Food Chem.* **2012**, *60*, 7297–7305. [[CrossRef](#)]
14. Wang, F.X.; Wang, W.; Huang, Y.L.; Liu, Z.W.; Zhang, J. Characterization of a novel polysaccharide purified from a herb of *Cynomorium songaricum* Rupr. *Food Hydrocoll.* **2015**, *47*, 79–86. [[CrossRef](#)]
15. Tuvaanjav, S.; Han, S.Q.; Komata, M.; Ma, C.J.; Kanamoto, T.; Nakashima, H.; Yoshida, T. Isolation and antiviral activity of water-soluble *Cynomorium songaricum* Rupr. polysaccharides. *J. Asian Nat. Prod. Res.* **2016**, *18*, 159–171. [[CrossRef](#)]
16. Wang, F.X.; Liu, Q.; Wang, W.; Li, X.B.; Zhang, J. A polysaccharide isolated from *Cynomorium songaricum* Rupr. protects pc12 cells against H₂O₂-induced injury. *Int. J. Biomacro.* **2016**, *87*, 222–228. [[CrossRef](#)]
17. Dong, Q.; Hu, H.; Suo, Y.R.; Chi, X.F.; Wang, H.L. The complete chloroplast genome sequences of two species from *Nitraria*. *Mitochondrial DNA B* **2019**, *4*, 1229–1230. [[CrossRef](#)]
18. Chinese Academy of Sciences, China Flora Editorial Committee. *Flora Reipublicae Popularis Sinicae*; Science Press: Beijing, China, 1998; Volume 43, pp. 117–118.
19. Guo, Y.H.; Lin, H.M.; Lin, Z.J. Study on Identification Characteristics of *Cynomorium* of the *Nitraia Siberian*. *Gansu Agric. Sci. Technol.* **2010**, *3*, 15–17.
20. Chen, Y.; Han, D.H.; Gao, H.; Luo, G.H.; Wang, J. Distribution and Utilization on Germplasm Resources of Host Plants of *Cynomorium songaricum*. *Chin. Wild Plant Resour.* **2013**, *32*, 45–47.
21. Chinese Academy of Sciences; China Flora Editorial Committee. *Flora Qinghaiica*; Qinghai People's Publishing House: Xinning, China, 1999; Volume 2, pp. 289–290.
22. Pan, X.Y.; Cao, Q.D.; Wei, Q.S.; Wang, G.X. Progress of researches on systematic and biodiversity in the genus *Nitraria* L. *Chin. Acad. Med. Organ.* **2002**, *4*, 1–6.
23. Chun, L.; Zhao, S.Z.; Hao, Y.Z.; Hu, Z.M.; Ma, Y.H. The resources and applications of *Nitraria* L. *Chin. Wild Plant Resour.* **2016**, *35*, 58–60.
24. Ren, J.; Tao, L. Numerical analysis on the growth benefits of the genus *Nitraria*. *J. Gansu Agric. Univ.* **2001**, *36*, 130–134.
25. Wu, C.R.; Li, Y.; Zhang, X.Q.; Xiao, B. Study on adaptability of *Nitraria* seedlings to salt stress. *Gansu Sci. Technol.* **2009**, *25*, 154–155.
26. Li, T.C.; Suo, Y.R. Characteristic of Trace Elements in Plant *Nitraria* Leaf from Qinghai Chaidamu Region. *Guangdong Trace Elements Sci.* **2002**, *9*, 66–68.
27. Liu, L.P. Analysis and appraisal on nutritional components of the four plants of *Nitraria* in Inner Mongolia. Master's Thesis, Inner Mongolia Agricultural University, Inner Mongolia, China, May 2009.
28. Liu, L.P.; Si, Q.B.L.G.; Xu, Z.M.; He, Z. Nutritional Components of Fruits of *Nitraria* L. and Its Utilization in Alashan Desert Area. *J. Inner Mongolia Forestry Sci Tech.* **2016**, *42*, 29–31.
29. Wang, S.X.; Li, Q.H.; Xu, J.; Gao, T.T.; Xin, Z.M. Experimental research on the pollination characteristics of 4 plant species of genus *Nitraria* L. *J. Biol.* **2012**, *29*, 49–51.
30. Zhou, L.B. Factor Analysis and Cluster Analysis on Trace Elements in *Nitraria* Leaf in Qinghai Area. *J. Anhui Agric. Sci.* **2010**, *38*, 10360–10361.

31. Cui, J.Y.; Vijayakumar, V.; Zhang, G. Partitioning of Fungal Endophyte Assemblages in Root-Parasitic Plant *Cynomorium songaricum* and Its Host *Nitraria tangutorum*. *Front. Microbiol.* **2018**, *9*, 666. [[CrossRef](#)] [[PubMed](#)]
32. Smeekens, S.; Ma, J.K.; Hanson, J.; Hanson, J.; Rolland, F. Sugar signals and molecular networks controlling plant growth. *Curr. Opin. Plant Biol.* **2010**, *13*, 274–279. [[CrossRef](#)]
33. Pan, L.; Cai, C.; Liu, C.J.; Liu, D.; Li, G.Y.; Linhardt, R.J.; Yu, G.L. Recent progress and advanced technology in carbohydrate-based drug development. *Curr. Opin. Biotechnol.* **2021**, *69*, 191–198. [[CrossRef](#)]
34. Gaudet, P.; Livstone, M.S.; Lewis, S.E.; Thomas, P.D. Phylogenetic-based propagation of functional annotations within the Gene Ontology consortium. *Brief. Bioinform.* **2011**, *12*, 449–462. [[CrossRef](#)] [[PubMed](#)]
35. Harrison, C.J.; Mould, R.M.; Leech, M.J.; Johnson, S.A.; Turner, L.; Schreck, S.L.; Baird, K.M.; Jack, P.L.; Rawsthorne, S.; Hedley, C.L.; et al. The rug3 locus of pea encodes plastidial phosphoglucomutase. *Plant Physiol.* **2000**, *122*, 1187–1192. [[CrossRef](#)] [[PubMed](#)]
36. Meng, M.; Geisler, M.; Johansson, H.; Harholt, J.; Scheller, H.V.; Mellerowicz, E.J.; Kleczkowski, L.A. UDP-glucose pyrophosphorylase is not rate limiting, but is essential in *Arabidopsis*. *Plant Cell Physiol.* **2009**, *50*, 998–1011. [[CrossRef](#)]
37. Park, J.I.; Ishimizu, T.; Suwabe, K.; Sudo, K.; Masuko, H.; Hakozaiki, H.; Nou, I.S.; Suzuki, G.; Watanabe, M. UDP-glucose pyrophosphorylase is rate limiting in vegetative and reproductive phases in *Arabidopsis thaliana*. *Plant Cell Physiol.* **2010**, *51*, 981–996. [[CrossRef](#)]
38. Dilokpimol, A.; Poulsen, C.P.; Vereb, G.; Kaneko, S.; Schulz, A.; Geshi, N. Galactosyltransferases from *Arabidopsis thaliana* in the biosynthesis of type II arabinogalactan: Molecular interaction enhances enzyme activity. *BMC Plant Biol.* **2014**, *14*, 90. [[CrossRef](#)]
39. Knoch, E.; Dilokpimol, A.; Tryfona, T.; Poulsen, C.P.; Xiong, G.; Harholt, J.; Petersen, B.L.; Ulvskov, P.; Hadi, M.Z.; Kotake, T.; et al. A beta-glucuronosyltransferase from *Arabidopsis thaliana* involved in biosynthesis of type II arabinogalactan has a role in cell elongation during seedling growth. *Plant J.* **2013**, *76*, 1016–1029. [[CrossRef](#)] [[PubMed](#)]
40. Qin, C.; Qian, W.Q.; Wang, W.F.; Wu, Y.; Yu, C.M.; Jiang, X.H.; Wang, D.W.; Wu, P. GDP-mannose pyrophosphorylase is a genetic determinant of ammonium sensitivity in *Arabidopsis thaliana*. *Proc. Natl. Acad. Sci. USA* **2008**, *105*, 18308–18313. [[CrossRef](#)] [[PubMed](#)]
41. Bonin, C.P.; Freshour, G.; Hahn, M.G.; Vanzin, G.F.; Reiter, W.D. The GMD1 and GMD2 genes of *Arabidopsis* encode isoforms of GDP-D-mannose 4,6-dehydratase with cell type-specific expression patterns. *Plant Physiol.* **2003**, *132*, 883–892. [[CrossRef](#)] [[PubMed](#)]
42. Filichkin, S.A.; Leonard, J.M.; Monteros, A.; Liu, P.P.; Nonogaki, H. A novel endo-beta-mannanase gene in tomato LeMAN5 is associated with anther and pollen development. *Plant Physiol.* **2004**, *134*, 1080–1087. [[CrossRef](#)] [[PubMed](#)]
43. Wang, Y.; Mortimer, J.C.; Davis, J.; Dupree, P.; Keegstra, K. Identification of an additional protein involved in mannan biosynthesis. *Plant J.* **2013**, *73*, 105–117. [[CrossRef](#)]
44. Maruta, T.; Yonemitsu, M.; Yabuta, Y.; Tamoi, M.; Ishikawa, T.; Shigeoka, S. *Arabidopsis* phosphomannose isomerase 1, but not phosphomannose isomerase 2, is essential for ascorbic acid biosynthesis. *J. Biol. Chem.* **2008**, *283*, 28842–28851. [[CrossRef](#)] [[PubMed](#)]
45. Halliday, J. Molecular analysis and functional elucidation of a novel plant O-fucosyltransferase in *Arabidopsis thaliana* and *Brassica napus*. Ph.D. Thesis, The University of Guelph, Ontario, Canada, June 2016.
46. Vogel, G.; Fiehn, O.; Jean-Richard-dit-Bressel, L.; Boller, T.; Wiemken, A.; Aeschbacher, R.A.; Winkler, A. Trehalose metabolism in *Arabidopsis*: Occurrence of trehalose and molecular cloning and characterization of trehalose-6-phosphate synthase homologues. *J. Exp. Bot.* **2001**, *52*, 1817–1826. [[CrossRef](#)]
47. De Coninck, B.; Le Roy, K.; Francis, I.; Clerens, S.; Vergauwen, R.; Halliday, A.M.; Smith, S.M.; Van Laere, A.; Van Den Ende, W. *Arabidopsis* AtcwINV3 and 6 are not invertases but are fructan exohydrolases (FEHs) with different substrate specificities. *Plant Cell Environ.* **2005**, *28*, 432–443. [[CrossRef](#)]
48. Le Roy, K.; Lammens, W.; Verhaest, M.; De Coninck, B.; Rabijns, A.; Van Laere, A.; Van den Ende, W. Unraveling the difference between invertases and fructan exohydrolases: A single amino acid (Asp-239) substitution transforms *Arabidopsis* cell wall invertase1 into a fructan 1-exohydrolase. *Plant Physiol.* **2007**, *145*, 616–625. [[CrossRef](#)]
49. Cho, Y.H.; Yoo, S.D. Signaling role of fructose mediated by FINS1/FBP in *Arabidopsis thaliana*. *PLoS Genet.* **2011**, *7*, e1001263. [[CrossRef](#)]
50. Berrocal-Lobo, M.; Ibanez, C.; Acebo, P.; Ramos, A.; Perez-Solis, E.; Collada, C.; Casado, R.; Aragoncillo, C.; Allona, I. Identification of a homolog of *Arabidopsis* DSP4 (SEX4) in chestnut: Its induction and accumulation in stem amyloplasts during winter or in response to the cold. *Plant Cell Environ.* **2011**, *34*, 1693–1704. [[CrossRef](#)]
51. Paparelli, E.; Gonzali, S.; Parlanti, S.; Novi, G.; Giorgi, F.M.; Licausi, F.; Kosmacz, M.; Feil, R.; Lunn, J.E.; Brust, H.; et al. Misexpression of a chloroplast aspartyl protease leads to severe growth defects and alters carbohydrate metabolism in *Arabidopsis*. *Plant Physiol.* **2012**, *160*, 1237–1250. [[CrossRef](#)]
52. Dumez, S.; Wattedled, F.; Dauvillee, D.; Delvalle, D.; Planchot, V.; Ball, S.G.; D’Hulst, C. Mutants of *Arabidopsis* lacking starch branching enzyme II substitute plastidial starch synthesis by cytoplasmic maltose accumulation. *Plant Cell* **2006**, *18*, 2694–2709. [[CrossRef](#)] [[PubMed](#)]
53. Kossmann, J.; Abel, G.J.W.; Springer, F.; Lloyd, J.R.; Willmitzer, L. Cloning and functional analysis of a cDNA encoding a starch synthase from potato (*Solanum tuberosum* L.) that is predominantly expressed in leaf tissue. *Planta* **1999**, *208*, 503–511. [[CrossRef](#)]
54. Arms, K.; Camp, P.S. *Biology*, 4th ed.; Saunders College publishing: Philadelphia, PA, USA, 2010; pp. 929–946.

55. Johnson, D.A.; Hill, J.P.; Thomas, M.A. The monosaccharide transporter gene family in land plants is ancient and shows differential subfamily expression and expansion across lineages. *BMC Evol. Biol.* **2006**, *6*, 64.
56. Kiyosue, T.; Abe, H.; Yamaguchi-Shinozaki, K.; Shinozaki, K. ERD6, a cDNA clone for an early dehydration-induced gene of *Arabidopsis*, encodes a putative sugar transporter. *Biochim. Biophys. Acta.* **1998**, *1370*, 187–191. [[CrossRef](#)]
57. Toyofuku, K.; Kasahara, M.; Yamaguchi, J. Characterization and expression of monosaccharide transporters (osMSTs) in rice. *Plant Cell Physiol.* **2000**, *41*, 940–947. [[CrossRef](#)]
58. Sherson, S.M.; Hemmann, G.; Wallace, G.; Forbes, S.; Germain, V.; Stadler, R.; Bechtold, N.; Sauer, N.; Smith, S.M. Monosaccharide/proton symporter AtSTP1 plays a major role in uptake and response of *Arabidopsis* seeds and seedlings to sugars. *Plant J.* **2000**, *24*, 849–857. [[CrossRef](#)] [[PubMed](#)]
59. Eom, J.S.; Chen, L.Q.; Sosso, D.; Julius, B.T.; Lin, I.W.; Qu, X.Q.; Braun, D.M.; Frommer, W.B. SWEETs, transporters for intracellular and intercellular sugar translocation. *Curr. Opin. Plant Biol.* **2015**, *25*, 53–62. [[CrossRef](#)]
60. Chen, L.Q.; Qu, X.Q.; Hou, B.H.; Sosso, D.; Osorio, S.; Fernie, A.R.; Frommer, W.B. Sucrose efflux mediated by SWEET proteins as a key step for phloem transport. *Science* **2012**, *335*, 207–211. [[CrossRef](#)]
61. Ebert, B.; Rautengarten, C.; Guo, X.Y.; Xiong, G.Y.; Stonebloom, S.; Smith-Moritz, A.M.; Herter, T.; Chan, L.J.G.; Adams, P.D.; Petzold, C.J.; et al. Identification and characterization of a Golgi-localized UDP-xylose transporter family from *Arabidopsis*. *Plant Cell* **2015**, *27*, 1218–1227. [[CrossRef](#)]
62. Dubois, M.; Gilles, K.A.; Hamilton, J.K.; Rebers, P.A.; Smith, F. Colorimetric method for determination of sugars and related substances. *Anal. Chem.* **1956**, *28*, 350–356. [[CrossRef](#)]
63. Li, M.F.; Liu, X.Z.; Wei, J.H.; Zhang, Z.; Chen, S.J.; Liu, Z.H.; Xing, H. Selection of high altitude planting area of *Angelica sinensis* based on biomass, bioactive compounds accumulation and antioxidant capacity. *Chin. Tradit. Herb. Drugs* **2020**, *51*, 474–481.
64. Arnao, M.B. Some methodological problems in the determination of antioxidant activity using chromogen radicals: A practical case. *Trends Food Sci. Technol.* **2000**, *11*, 419–421. [[CrossRef](#)]
65. Li, M.F.; Pare, P.W.; Zhang, J.L.; Kang, T.L.; Zhang, Z.; Yang, D.L.; Wang, K.P.; Xing, H. Antioxidant capacity connection with phenolic and flavonoid content in Chinese medicinal herbs. *Rec. Nat. Prod.* **2018**, *3*, 239–250. [[CrossRef](#)]
66. Nencini, C.; Menchiari, A.; Franchi, G.G.; Micheli, L. In vitro antioxidant activity of aged extracts of some Italian *Allium* species. *Plant Foods Hum. Nutr.* **2011**, *66*, 11–16. [[CrossRef](#)]
67. Benzie, I.F.F.; Strain, J.J. The ferric reducing ability of plasma (FRAP) as a measure of antioxidant power: The FRAP assay. *Anal. Biochem.* **1996**, *239*, 70–76. [[CrossRef](#)] [[PubMed](#)]
68. Li, M.F.; Sun, P.; Kang, T.L.; Xing, H.; Yang, D.L.; Zhang, J.L.; Paré, P.W. Mapping podophyllotoxin biosynthesis and growth-related transcripts with high elevation in *Sinopodophyllum hexandrum*. *Ind. Crop* **2018**, *124*, 510–518. [[CrossRef](#)]
69. Grabherr, M.G.; Haas, B.J.; Yassour, M.; Levin, J.Z.; Thompson, D.A.; Amit, I.; Adiconis, X.; Fan, L.; Raychowdhury, R.; Zeng, Q.D.; et al. Full-length transcriptome assembly from RNA-Seq data without a reference genome. *Nat. Biotechnol.* **2011**, *29*, 644–652. [[CrossRef](#)] [[PubMed](#)]
70. Mortazavi, A.; Williams, B.A.; McCue, K.; Schaeffer, L.; Wold, B. Mapping and quantifying mammalian transcriptomes by RNA-Seq. *Nat. Methods* **2008**, *5*, 621–628. [[CrossRef](#)] [[PubMed](#)]
71. Love, M.I.; Huber, W.; Anders, S. Moderated estimation of fold change and dispersion for RNAseq data with DESeq2. *Genome Biol.* **2014**, *15*, 550. [[CrossRef](#)] [[PubMed](#)]
72. Robinson, M.D.; McCarthy, D.J.; Smyth, G.K. EdgeR: A Bioconductor package for differential expression analysis of digital gene expression data. *Brief Bioinform.* **2010**, *26*, 139–140. [[CrossRef](#)]
73. Conesa, A.; Götz, S.; García-Gómez, J.M.; Terol, J.; Talón, M.; Robles, M. Blast2GO: A universal tool for annotation, visualization and analysis in functional genomics research. *Brief Bioinform.* **2005**, *21*, 3674–3676. [[CrossRef](#)] [[PubMed](#)]
74. Willems, E.; Leyns, L.; Vandesompele, J. Standardization of real-time PCR gene expression data from independent biological replicates. *Anal. Biochem.* **2008**, *379*, 127–129. [[CrossRef](#)]